International Journal on Magnetic Particle Imaging
Vol 6, No 1, Article ID 2003003, 8 Pages

Infinite Science Publishing

Research Article

Magnetic Particle Imaging Using Discrete Sampling and Image Reconstruction with Few Orthogonal Bases Obtained by Singular Value Decomposition of Selected Delta Responses

Yushi Ono[a,*] · Yasutoshi Ishihara[b]

[a] Graduate School of Science and Technology, Meiji University, Kawasaki, Japan
[b] School of Science and Technology, Meiji University, Kawasaki, Japan
*Corresponding author, email: ce182018@meiji.ac.jp

Received 18 May 2019; Accepted 23 December 2019; Published online 28 March 2020

Abstract

The conventional magnetic particle imaging reconstruction methods use observed signals and system functions, which result in an enormous amount of data and long processing time being required to reconstruct large image matrices. We propose a new image reconstruction method that uses less data and a limited number of orthogonal bases obtained via the singular value decomposition (SVD) of selected point spread functions (PSFs). By using the features of the diagonal and nondiagonal elements of a singular value matrix, image blurring and artifacts can be reduced in the reconstructed image. This is because the diagonal components commonly indicate the similarities between each orthogonal basis for the system function and an observed signal, whereas the nondiagonal components indicate the differences of both them. In this paper, we use numerical analyses to demonstrate that image reconstruction is possible by using effective orthogonal bases obtained through the SVD of a limited number of PSFs selected from a general system function. The reconstruction time is reduced to 1/12th to 1/50th of that of the conventional method.

I. Introduction

Magnetic particle imaging (MPI) has been proposed as a medical imaging technology that facilitates the early diagnosis of serious illnesses such as cancer or cardiovascular diseases [1]. In the conventional MPI reconstruction methods, the magnetic nanoparticle (MNP) distribution is typically reconstructed by applying an inverse problem analysis to a system function and observed signals [2]. In contrast, in a previous work, we had proposed an image reconstruction method that uses orthogonal bases derived from singular value decomposition (SVD) [3, 4]. In our method, SVD was used to expand the individual delta responses (in the following text, they are refered to as point spread functions (PSFs)) used to generate the system functions obtained from the MNPs, which were arranged at each matrix position of an image.

By using such expanded system functions and focusing on the diagonal and nondiagonal elements of the singular value matrix, reduction in image blurring and artifacts could be achieved, resulting in improved image

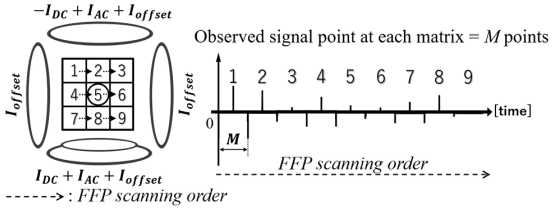

Figure 1: Observed signal detected via discrete FFP scans.

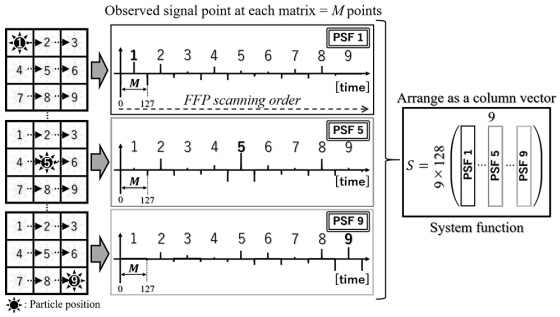

Figure 2: Definition of the general system function.

resolution. This was because the diagonal components commonly indicated the similarities between each PSF and an observed signal, whereas, the nondiagonal components indicated the differences between both, with high sensitivity. We had focused on these properties and applied them to the field of pattern recognition [5]. Recently, an applied research using a similar signal processing technique was reported in the field of abnormal waveform detection [6]. By using these concepts, it was possible to reconstruct an MPI image with high image resolution and high image-signal-to-noise ratio. However, because system functions with redundant information were used, in both the conventional method and our previously proposed reconstruction method, the image reconstruction time could be considerably long, depending on the sizes of the image matrices.

Therefore, we attempted to examine how the number of orthogonal bases used for image reconstruction could be reduced without degrading the image quality. Recently, specific basis transformations such as the Fourier transform and the cosine transform, which can be used to sparsify the MPI system matrix, were reported to be highly effective for reducing the number of calibration scans and reconstruction procedures [7–10]. In contrast, in a previous work, we proposed a novel reconstruction method to select an arbitrary orthogonal basis from the system function comprising the set of all PSFs expanded via SVD [11]. In this study, we extend the previous work by performing numerical analyses to evaluate the quality of the reconstructed image obtained using the proposed methods. In particular, we propose a selection indicator to select the appropriate orthogonal bases necessary for reconstruction.

II. Materials and Methods

II.I. Scanning method for signal acquisition

In this study, we assume that signals are acquired using the classic field-free point (FFP) scanning procedure, to evaluate the effects caused by the image reconstruction method [12, 13]. That is, as shown in Figure 1, when acquiring magnetization signals generated from MNPs as induced electromotive forces (EMFs), the FFP is scanned discretely for each matrix position (1, 2, ..., 9 in Figure 1) by adjusting the offset current (I_{offset}) of a Maxwell coil. The observed signal is defined as a series of EMF signals detected over M time sampling points for each matrix position, by superimposing an alternating magnetic field on the FFPs. When compared to the 2D Lissajous scan, such a 1D discrete scan requires more time to acquire signal data; however, as mentioned above, we use a basic scanning method whose scan parameters seem to have little effect to examine the validity of the reconstruction algorithm.

II.II. Formulation of the conventional method

In the general forward problem, the observed signal $\vec{\mathbf{o}}$ from the particle arrangement $\vec{\mathbf{p}}$ can be expressed as in equation (1) [2]. According to the scanning method shown in Figure 1, a delta response is obtained for each point-like particle sample placed at an image matrix position. These functions have $N \times M$ data points. Thus, the system function S is defined as an $(N \times M) \times N$ matrix, as shown in Figure 2, because it is a set of PSFs collected for the point-like particle samples placed at each of the N image matrix positions.

$$\vec{\mathbf{o}} = S\vec{\mathbf{p}} \tag{1}$$

The unknown particle arrangements $\vec{\mathbf{p}}$' can be estimated by applying the inverse problem procedure:

$$\vec{\mathbf{p}}' = (S^T S + \lambda I)^{-1} S^T \vec{\mathbf{o}} = V(\Sigma^T \Sigma + \lambda I)^{-1} V^T S^T \vec{\mathbf{o}}, \tag{2}$$

where V is the right-singular vector of the SVD, V^T is the transpose of matrix V, Σ contains the singular values, Σ^T is the transpose of matrix Σ, λ represents the normalized parameters, and S^T is the transpose of matrix S. An advantage of this method is that blurs and artifacts are unlikely to appear in the reconstructed image. However, as the matrix size increases, the image reconstruction time increases significantly. Therefore, in this study, we propose an image reconstruction method based on a

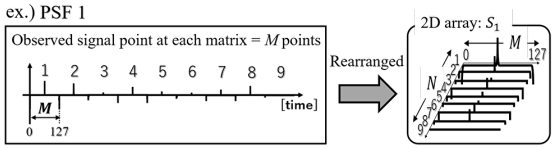

Figure 3: Definition of a PSF as a 2D array.

limited combination of PSFs instead of using a system function composed of all PSFs collected at all image matrix positions.

II.III. Concept of the proposed method

In general, SVD involves calculating the orthogonal basis that represents a target matrix most appropriately. Therefore, the orthogonal basis obtained via SVD, for a normal system function, is not universal for all matrices and often includes redundant components. Thus, in this paper, the system function is defined as a combination of several PSFs obtained from the MNPs arranged at each matrix position of an image. Although each PSF in Figure 2 can also be defined as a cascaded connection of signals observed when applying an alternating magnetic field while altering the position of an FFP when an MNP is arranged at the appropriate image matrix position, each PSF can be rearranged as a 2D array, as shown in Figure 3, for our formulation described below.

The procedure of the proposed method is described below, in four steps, and a schematic diagram is shown in Figure 4.

Step I

Each PSF is decomposed via SVD as

$$S_i = U_i \Sigma_i V_i^T, (i = 1, 2, \ldots, N), \tag{3}$$

where S_i is a 2D array of the rearranged 1D PSF defined in Figure 3 at the i^{th} image matrix position, and N is the total number of image matrix positions. Although this 2D array size is arbitrary to satisfy the total data number $(N \cdot M)$ of the PSF, it is typically comprises N rows and M columns. U_i is the left-singular vector, Σ_i is the singular value matrix, V_i is the right-singular vector, and V_i^T is the transpose of matrix V_i.

Step II

The basis used for orthogonal expansion is reduced from the left and right singular vectors. From the characteristics of SVD, the low-order orthogonal bases obtained from the left and right singular vectors contain several signals from the original PSF. By expressing the signal of the PSF with a low-order orthogonal basis, orthogonal expansion can be performed with a minimal number of

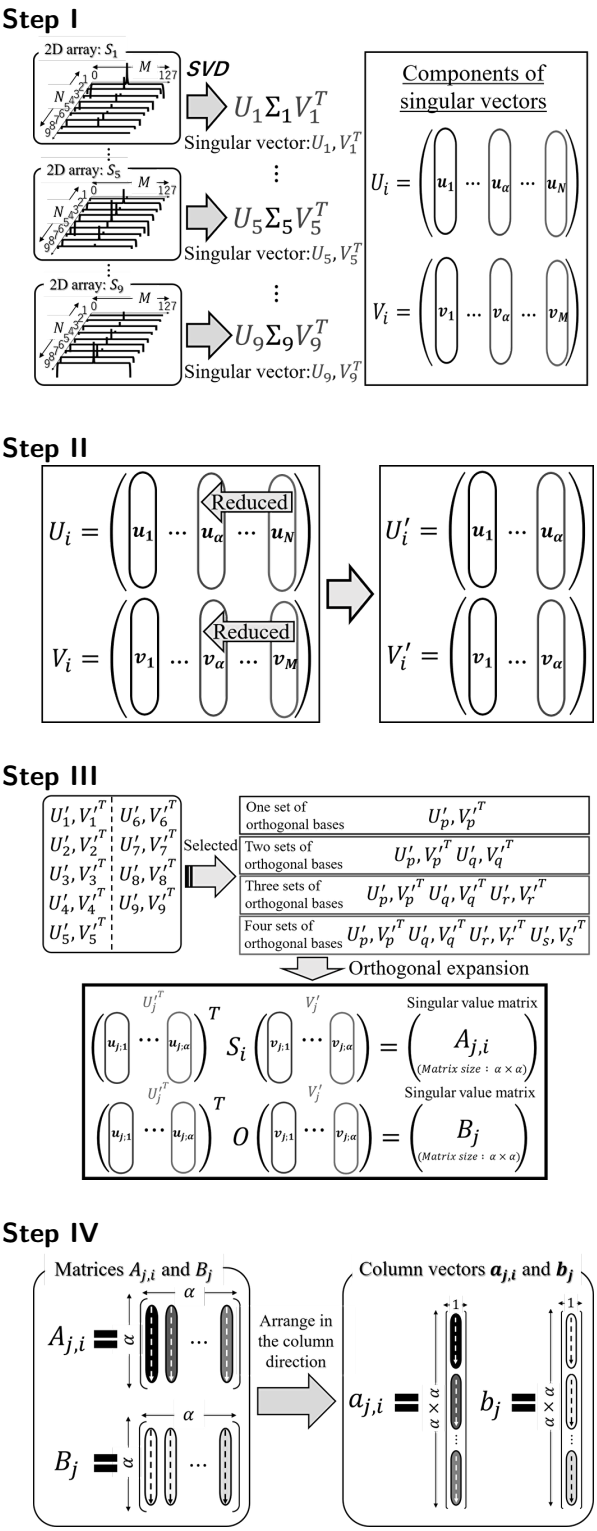

Figure 4: Procedure of the proposed method.

orthogonal bases. In particular, the orthogonal bases obtained via SVD can represent the original observed signal with fewer bases, than the case using bases such as the cosine transform, because the target data can be expanded very efficiently. Via this operation, U_i and V_i

are replaced by the reduced singular vectors U'_i and V'_i, respectively. The criterion for determining the number of orthogonal bases is described in the next section.

Step III

In this study, instead of using all N sets of orthogonal bases, one to four sets of orthogonal bases are selected and used for expanding the observed signals orthogonally. An orthogonal expansion using four sets of orthogonal bases $(U'_p, V'_p, U'_q, V'_q, U'_r, V'_r, U'_s, V'_s)$ is shown below as an example. The characteristic concept of our image reconstruction method is to newly expand each system function S_i with the orthogonal vectors U'_j and V'_j, which are obtained by expanding other system functions:

$$A_{j,i} = U_{j'}^T S_i V'_j,$$
$$(j = p, q, r, s(1 \le p < q < r < s \le N)), (i \ne j) \quad (4)$$

$$U_j'^T = (\mathbf{u}_{j;1} \cdots \mathbf{u}_{j;\alpha})^T, 1 \le \alpha \le N$$
$$(U_j'^T U'_j = I_\alpha) \quad (5)$$

$$V_j'^T = (\mathbf{v}_{j;1} \cdots \mathbf{v}_{j;\alpha})^T, 1 \le \alpha \le M$$
$$(V_j'^T V'_j = I_\alpha). \quad (6)$$

Here, $A_{j,i}$ is the singular value matrix, j is the number of sets of orthogonal bases, U'^T_j is the left inverse of U'^T_i, V'_i is the right inverse of V'^T_j, $\mathbf{u}_{j;\alpha}$ is the α^{th} left-singular vector, $\mathbf{v}_{j;\alpha}$ is the α^{th} right-singular vector, α denotes the selected column vector, and I_α is an identity matrix. When the PSF 2D array S_i is expanded using the orthogonal bases U'_j and V'_j, the singular value matrix Σ_i is reduced to only the diagonal elements, whereas, the difference between S_j and S_i is reflected in the singular vector matrix $A_{j,i}$ as diagonal and nondiagonal elements. If the information of $A_{j,i}$ is used efficiently, image reconstruction may be possible using only a few orthogonal bases. Furthermore, by using the same orthogonal bases U'_j and V'_j, the observed signals O obtained from the unknown MNP distributions can be expanded orthogonally, and the singular value matrix B_j can be calculated as

$$B_j = U_j'^T O V'_j. \quad (7)$$

Step IV

When matrices $A_{j,i}$ and B_j obtained via orthogonal expansion are organized as column vectors $\mathbf{a_{j,i}}$ and $\mathbf{b_j}$ $((i = 1, 2, \ldots, N), (j = p, q, r, s\,(1 \le p < q < r < s \le N)))$, respectively, the following equation holds:

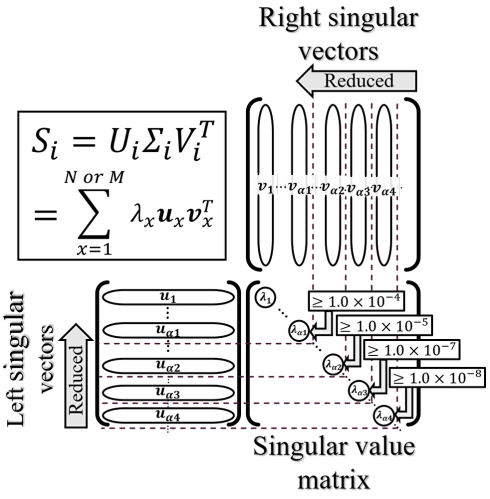

Figure 5: Reduction of orthogonal bases.

$$\begin{pmatrix} \mathbf{b}_p \\ \mathbf{b}_q \\ \mathbf{b}_r \\ \mathbf{b}_s \end{pmatrix} = \begin{pmatrix} \mathbf{a}_{p,1} & \cdots & \mathbf{a}_{p,N} \\ \mathbf{a}_{q,1} & \cdots & \mathbf{a}_{q,N} \\ \mathbf{a}_{r,1} & \cdots & \mathbf{a}_{r,N} \\ \mathbf{a}_{s,1} & \cdots & \mathbf{a}_{s,N} \end{pmatrix} \vec{\mathbf{p}}, \quad (8)$$

where $\vec{\mathbf{p}}^{N\times 1}$ is the MNP arrangement. Similar to equation (2), an image is reconstructed by applying an inverse problem analysis to equation (8) to calculate the unknown particle arrangement $\vec{\mathbf{p}}'$.

II.IV. Reduction of orthogonal bases

In principle, if orthogonal expansion is performed using all the left and right singular vectors obtained by SVD, the original image can be reconstructed without error. However, because it is obvious that the amount of data will be enormous, it is desirable to perform orthogonal expansions with the minimum number of singular vectors, for image reconstruction. Thus, in this study, we investigated the criteria for selecting the reduced orthogonal bases required for image reconstruction. According to equations (5) and (6) shown in Step III described above, the left and right singular vectors are reduced from the high-order singular vectors, as shown in Figure 5, and image reconstruction is performed using such minimal data. Here, the following four conditions (a) to (d) are used as thresholds for determining the order of the vectors to be used, based on the singular values obtained when SVD is applied to the central PSF (the percentages listed indicate the rates of the orthogonal bases actually used with respect to the numbers of orthogonal bases when all the PSFs are used). The reason for using the singular value for the central PSF as the threshold criterion is that, approximating the original waveform of

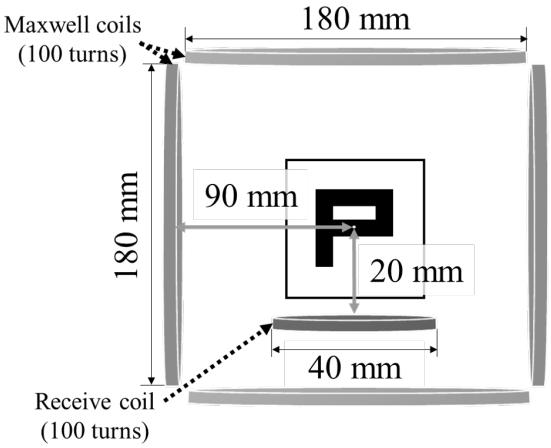

Figure 6: Analysis conditions and ideal MNP position.

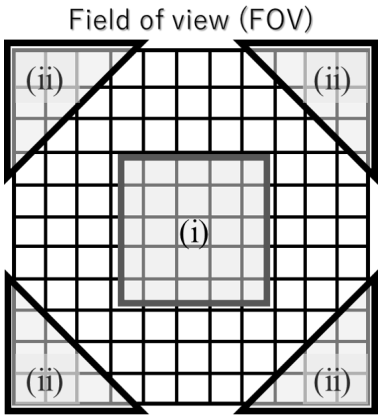

Figure 7: Selection regions of orthogonal bases.

the central PSF tends to require more vectors than approximating the original waveform of the PSF at other positions.

(a) $\lambda_{\alpha 1} \geq 1.0 \cdot 10^{-4}$ (7.4 %) (9 right and left vectors)

(b) $\lambda_{\alpha 2} \geq 1.0 \cdot 10^{-5}$ (12.4 %) (15 right and left vectors)

(c) $\lambda_{\alpha 3} \geq 1.0 \cdot 10^{-7}$ (18.2 %) (22 right and left vectors)

(d) $\lambda_{\alpha 4} \geq 1.0 \cdot 10^{-8}$ (20.7 %) (25 right and left vectors)

II.V. Conditions of numerical analysis

To validate the effectiveness of the proposed method, we performed numerical experiments. The field of view (FOV) was set to 30 mm × 30 mm with a matrix size of 11 × 11. A gradient magnetic field of 2.0 T m^{-1} was generated, and a sinusoidal alternating magnetic field of 20 mT was applied at a frequency of 122 Hz. MNPs with a particle size of 20 nm assuming an MNP made of ferucarbotran [13] were arranged as shown in Figure 6. The observed signal was calculated assuming the Langevin model, but the relaxation term was ignored because of the low frequency of the alternating magnetic field used. Additionally, the number of sampling points for the observed signal generated from the MNPs was 128. All numerical analyses were performed on a PC (Intel Core i5-7200U with 2.50 GHz and 8 GB DDR3 RAM) using a C language program, and the singular values were calculated using a general algorithm described in "Numerical Recipes in C" [14]. To perform image reconstruction with as few orthogonal bases as possible, in this study, the number of left and right singular vectors was reduced; and one to four sets of the orthogonal bases used for orthogonal expansion were selected from 121 original PSFs, as described in Step III. At this point, the orthogonal bases used for image reconstruction were calculated based on the PSFs selected from the following two regions, which are shown in Figure 7:

(i) From the orthogonal bases of one to four PSFs near the center of the FOV.

(ii) From the orthogonal bases of one to four PSFs around the edges of the FOV. In this case, two or more orthogonal bases were not selected from the same area, among the four areas in Figure 7 (ii).

We examined the effects of the number of singular vectors and the sets of orthogonal bases on the reconstructed images, using both a subjective evaluation of the reconstructed images and an objective evaluation based on the mean squared error (MSE) values of the reconstructed images. In addition, a conventional inverse problem image reconstruction method was also used for comparison with these results. In both methods, image reconstruction was performed using the regularization parameter in inverse problem analysis, but no noise was considered in the analyses.

III. Results

Table 1 shows the images reconstructed via the proposed method and the MSE values for the singular value conditions (a) to (d), under which image reconstruction was clearly possible. The gray scale bar shows the normalized image intensity. Table 2 shows the calculation time required for each image reconstruction, under different conditions. In the calculation times shown in the table, the time shown for the conventional method corresponds to the image reconstruction time, whereas, the times shown for the proposed method correspond to the sum of the image reconstruction time and the time required to orthogonally expand the observed signal with the orthogonal basis.

The reconstructed images in Table 1 indicate that image reconstruction is possible by setting the conditions appropriately. Furthermore, from the results shown in Table 1, it can be seen that the orders of the MSE values are all smaller than 10^{-2}. Although the image quality is

Table 1: Results of reconstructed images.

Set of orthogonal bases	Selection region of orthogonal bases	Singular value conditions (a) $\geq 1.0 \cdot 10^{-4}$ (9 vectors)	(b) $\geq 1.0 \cdot 10^{-5}$ (15 vectors)	(c) $\geq 1.0 \cdot 10^{-7}$ (22 vectors)	(d) $\geq 1.0 \cdot 10^{-8}$ (25 vectors)
One set	(i)	 MSE: N/A	 MSE: N/A	 MSE: N/A	 MSE: N/A
	(ii)	 MSE: N/A	 MSE: N/A	 MSE: N/A	 MSE: N/A
Two sets	(i)	 MSE: N/A	 MSE: $4.12 \cdot 10^{-2}$	 MSE: $3.36 \cdot 10^{-2}$	 MSE: $3.26 \cdot 10^{-2}$
	(ii)	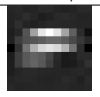 MSE: N/A	 MSE: $3.06 \cdot 10^{-2}$	 MSE: $2.89 \cdot 10^{-2}$	 MSE: $2.55 \cdot 10^{-2}$
Three sets	(i)	 MSE: N/A	 MSE: $4.13 \cdot 10^{-2}$	 MSE: $3.62 \cdot 10^{-2}$	 MSE: $3.50 \cdot 10^{-2}$
	(ii)	 MSE: N/A	 MSE: $2.87 \cdot 10^{-2}$	 MSE: $3.02 \cdot 10^{-2}$	 MSE: $2.64 \cdot 10^{-2}$
Four sets	(i)	 MSE: N/A	 MSE: $2.98 \cdot 10^{-2}$	 MSE: $3.02 \cdot 10^{-2}$	 MSE: $3.03 \cdot 10^{-2}$
	(ii)	 MSE: N/A	 MSE: $2.66 \cdot 10^{-2}$	 MSE: $2.87 \cdot 10^{-2}$	 MSE: $2.54 \cdot 10^{-2}$
Conventional inverse problem image reconstruction method		 MSE: $1.44 \cdot 10^{-2}$			 Image intensity

slightly inferior to that obtained via the conventional inverse problem image reconstruction method, it can be observed from Table 2 that the calculation time (i.e., the sum of the image reconstruction time and the time to orthogonally expand the observed signal with the orthogonal basis) is reduced significantly; it is approximately 50 times shorter at the most and 12 times shorter at the least.

IV. Discussion

First, we consider the reconstructed image quality and MSE values. Based on the results of the reconstructed image and by comparing the two conditions in Table 1, it can be seen that the image quality of the reconstructed image improves when increasing the number of orthogonal bases used for orthogonal expansion, as the threshold of the singular value decreases. That is, increasing the set of orthogonal bases improves the image quality and the result asymptotically approaches the results obtained using the conventional image reconstruction methods.

However, although the setting of the four threshold values (α_1-α_4) in this study reduces the number of orthogonal bases used for image reconstruction to 9, 15, 22, and 25, respectively, and shortens the reconstruction time correspondingly, the parameters should be selected appropriately, considering the required image quality and reconstruction time.

Moreover, to investigate which PSF's orthogonal basis leads to an improvement in image quality, the conditions near the center and edges are divided, and the

Table 2: Calculation time required for imaging.

Sets of orthogonal bases	Selection region of orthogonal bases	Singular value conditions (b) $\geq 1.0 \cdot 10^{-5}$ (15 vectors)	(c) $\geq 1.0 \cdot 10^{-7}$ (22 vectors)	(d) $\geq 1.0 \cdot 10^{-8}$ (25 vectors)
		Calculation time [s]		
Two sets	(i) (ii)	0.332	0.571	0.737
Three sets	(i) (ii)	0.490	0.873	1.080
Four sets	(i) (ii)	0.603	1.118	1.425
Conventional inverse problem image reconstruction method			17.122	

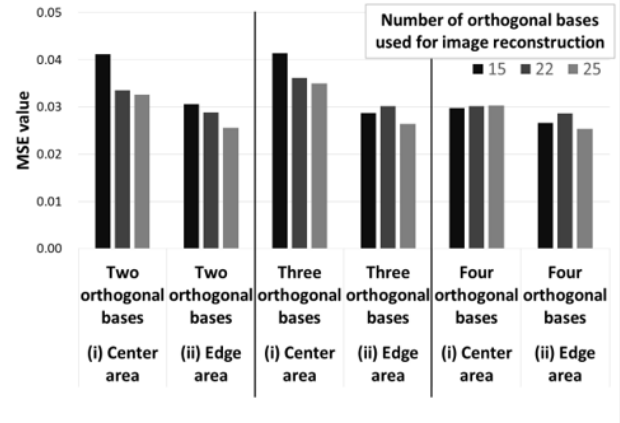

Figure 8: Comparison of MSE values.

MSE values obtained from the reconstructed image are compared, as shown in Figure 8. When comparing the MSE values, it can be seen that the PSF's orthogonal basis is better near the edges than near the center. However, when the number of orthogonal bases to be selected is increased or when the threshold value is lowered, the MSE values near the center and those near the edges tend to be almost identical. From these facts, when performing image reconstruction using a small number of orthogonal bases, the orthogonal bases obtained from PSFs near the edges are more important. However, as the number of orthogonal bases increases, the reconstructed images obtained using the center and edge orthogonal bases exhibit little difference in quality.

Although we proposed a reconstruction method using orthogonal bases by applying SVD to PSFs, in this paper, it has also been demonstrated that the system function can be expressed approximately by Chebyshev functions [15]. In fact, the orthogonal basis of each order obtained by SVD is almost equivalent to the Chebyshev basis in the frequency domain, under ideal conditions. Although it is necessary to discuss the error due to the various factors (i.e., particle type, drive-field waveform, field homogeneities and linearity, and so on) when we use Chebyshev polynomials whose orthogonal basis form is fixed for image reconstruction, the optimal orthogonal basis may be obtained individually even if SVD is applied to the signal data acquired under different conditions. Therefore, the proposed method may not be affected by the above error factors, and we will consider it in the future. In addition, by clarifying the similarities and differences between both orthogonal bases, it may be possible to indicate not only the magnitude of singular values but also a more rational selection criterion for the required orthogonal bases.

V. Conclusions

We proposed a new image reconstruction method using the orthogonal bases obtained by applying SVD to the PSFs. It was confirmed that image reconstruction was possible using a small number of column vectors for the right and left singular vectors. The results indicated that the image reconstruction time could be shortened significantly while suppressing the image quality deterioration. In a future work, we will clarify the number of orthogonal bases suitable for image reconstruction and the regions of the PSFs that should be selected. In addition, we do believe that the effects of noise should be evaluated, to demonstrate the practicality of this method.

Acknowledgement

This study was supported by a Designated Research Project (A), 2018, from the Institute of Science and Technology of Meiji University.

References

[1] B. Gleich and J. Weizenecker. Tomographic imaging using the nonlinear response of magnetic particles. *Nature*, 435(7046):1214–1217, 2005, doi:10.1038/nature03808.

[2] J. Weizenecker, J. Borgert, and B. Gleich. A simulation study on the resolution and sensitivity of magnetic particle imaging. *Physics in Medicine and Biology*, 52(21):6363–6374, 2007, doi:10.1088/0031-9155/52/21/001.

[3] T. Takagi, S. Shimizu, H. Tsuchiya, T. Hatsuda, T. Noguchi, and Y. Ishihara, Image reconstruction method based on orthonormal basis of observation signal by singular value decomposition for magnetic particle imaging, in *2015 5th International Workshop on Magnetic Particle Imaging (IWMPI)*, IEEE, 2015. doi:10.1109/IWMPI.2015.7107052.

[4] T. Takagi, H. Tsuchiya, T. Hatsuda, and Y. Ishihara. Image Reconstruction Method Using Orthonormal Basis by Singular Value Decomposition for Magnetic Particle Imaging. *Transactions of Japanese Society for Medical and Biological Engineering*, 53(5):276–282, 2015, doi:10.11239/jsmbe.53.276.

[5] Y. Ishihara and K. Mori, Magnetic resonance imaging, Japanese Patent, JPA 1994-86763, 1992.

[6] T. Idé and K. Tsuda, Change-Point Detection using Krylov Subspace Learning, in *Proceedings of the 2007 SIAM International Conference on Data Mining*, 515–520, Philadelphia, PA: Society for Industrial and Applied Mathematics, 2007. doi:10.1137/1.9781611972771.54.

[7] J. Lampe, C. Bassoy, J. Rahmer, J. Weizenecker, H. Voss, B. Gleich, and J. Borgert. Fast reconstruction in magnetic particle imaging. *Physics in Medicine and Biology*, 57(4):1113–1134, 2012, doi:10.1088/0031-9155/57/4/1113.

[8] T. Knopp and A. Weber. Sparse reconstruction of the magnetic particle imaging system matrix. *IEEE Transactions on Medical Imaging*, 32(8):1473–1480, 2013, doi:10.1109/TMI.2013.2258029.

[9] A. Weber and T. Knopp. Reconstruction of the Magnetic Particle Imaging System Matrix Using Symmetries and Compressed Sensing. *Advances in Mathematical Physics*, 2015, 2015, doi:10.1155/2015/460496.

[10] M. Maass, M. Ahlborg, A. Bakenecker, F. Katzberg, H. Phan, T. M. Buzug, and A. Mertins. A Trajectory Study for Obtaining MPI System Matrices in a Compressed-Sensing Framework. *International Journal on Magnetic Particle Imaging*, 3(2), 2017, doi:10.18416/IJMPI.2017.1706005.

[11] Y. Ono and Y. Ishihara, Image reconstruction method of magnetic particle imaging using orthogonality of singular value decomposition, in *International Workshop on Magnetic Particle Imaging*, 2019.

[12] Y. Ishihara, T. Kuwabara, T. Honma, and Y. Nakagawa. Correlation-Based Image Reconstruction Methods for Magnetic Particle Imaging. *IEICE Transactions on Information and Systems*, E95-D(3):872–879, 2012, doi:10.1587/transinf.E95.D.872.

[13] Y. Ishihara, T. Honma, S. Nohara, and Y. Ito. Evaluation of magnetic nanoparticle samples made from biocompatible ferucarbotran by time-correlation magnetic particle imaging reconstruction method. *BMC Medical Imaging*, 13(1):15, 2013, doi:10.1186/1471-2342-13-15.

[14] W. H. Press, S. A. Teukolsky, W. T. Vetterling, and B. P. Flannery, Numerical Recipes in C, Second edi. Cambridge University Press, 1992, ISBN: 0-521-43108-5.

[15] J. Rahmer, J. Weizenecker, B. Gleich, and J. Borgert. Signal encoding in magnetic particle imaging: properties of the system function. *BMC Medical Imaging*, 9:4, 2009, doi:10.1186/1471-2342-9-4.

